Facile Synthesis of Fluorescent Latex Nanoparticles with Selective Binding Properties Using Amphiphilic Glycosylated Polypeptide Surfactants

J. Jacobs,[†] A. Byrne,[†] N. Gathergood,[†] T. E. Keyes,[†] J. P. A. Heuts,[‡] and A. Heise*,[†,‡]

[†]School of Chemical Sciences, Dublin City University, Glasnevin, Dublin 9, Ireland

[‡]Department of Chemical Engineering and Chemistry, Eindhoven University of Technology, P.O. Box 513, 5600 MB Eindhoven, The Netherlands

Ⓢ *Supporting Information*

ABSTRACT: Block copolymers comprising a poly(styrene) and a poly(L-lysine) or poly(L-glutamic acid) block were obtained by sequential reversible addition−fragmentation chain Transfer (RAFT) and N-carboxyanhydride (NCA) polymerization. Subsequent partial glycosylation of the poly(L-glutamic acid) block with D-galactosamine (GA) and the poly(L-lysine) block with lactobionic acid (LA) yielded block copolymers with a degree of glycosylation of 50% and 35%, respectively, in the poly(amino acid) block. These amphiphilic block copolymers were successfully employed as macromolecular surfactants in the emulsion polymerization of styrene to produce uniform 100−150 nm size nanoparticles with a poly(syrene) core and galactose containing poly(L-amino acid) periphery. Introduction of fluorescence was achieved by incorporation of Nile Red during latex formation and reaction of remaining lysine functionalities on the nanoparticle periphery with fluorescein isothiocyanate (FITC). The availability of the galactose units at the nanoparticles surface for selective binding was demonstrated by lectin binding experiments and binding to Chinese hamster ovary (CHO) cells. Confocal images of live CHO cells following incubation with fluorescent glycosylated nanoparticles confirmed that the nanoparticles bound strongly to the cell surface and could only be removed by addition of free lactobionic acid, highlighting selective binding of the nanoparticles on the cell surface.
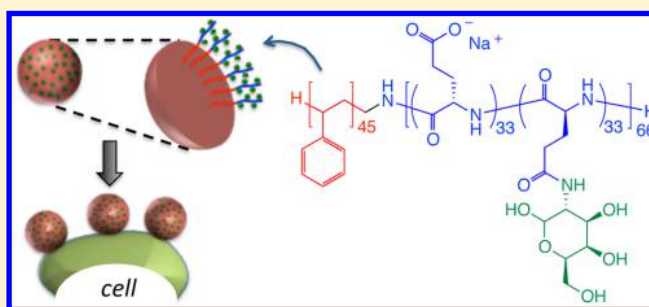
INTRODUCTION

The interest in advanced nanoparticles (NP) has significantly increased recently due to the technological demands from emerging applications in biomedical devices. In particular in the area of diagnostics, functional nanoparticles with high contrast imaging capabilities combined with highly specific targeting properties toward clinically relevant targets are sought.[1−4] Inorganic nanoparticles are well documented for these tasks where some examples include iron oxide nanoparticles (IONPs) as a contrast-enhancing agent of magnetic resonance imaging (MRI).[5−7] Fluorescent silica nanoparticles (FSNPs) are another example of inorganic optical probes whereby silica NPs are loaded with a fluorescent dye as probes for sensitive imaging of, for example, cancer cells.[8−10]

Polymer-based NPs offer a highly promising alternative to inorganic nanoparticles for medical applications.[4,11] Most reported examples of polymer NPs rely on the self-assembly of amphiphilic block copolymers into various three-dimensional nanostructures such as micelles, vesicles, rods, and worms.[12−14] One drawback of these structures is their dynamic nature, which could cause stability issues under application conditions. Moreover, protocols of self-assembly and functionalization often require multiple steps, which could compromise

scalability of the materials. Solid polymer NPs are a promising alternative as they combine characteristics of solid inorganic NPs with the synthetic variability of polymers. Poly(lactic-*co*-glycolic acid)s (PLGA) have already been utilized for NPs owing to their excellent biocompatibility and biodegradability.[15] As the core material, PLGA has been combined with poly(ethylene glycol) (PEG) for several systems where NPs are typically prepared via nanoprecipitation or emulsification.[16,17] Furthermore, nondegradable fluorescent polystyrene (PS) and poly(methyl methacrylate) NPs have also been investigated successfully offering higher long-term stability for *in vitro* and *in vivo* cell imaging.[18,19] In a specific example Landfester reported the synthesis of functional fluorescent polystyrene NPs by miniemulsion polymerization incorporating functional acrylates for colloidal stability and as potential handles for postmodification. Cell uptake was visualized by fluorescent spectroscopy.[19]

A critical aspect is in the design to produce NPs tailored to its final application. Size, shape, and surface properties are

parameters that need to be tuned as these are critical for *in vitro* and *in vivo* performance.[20,21] Furthermore, diagnostic agents need to be specific in the detection of compromised cells, and for this reason active targeting concepts are desirable. This involves the conjugation of targeting ligands to the exposed surface of NPs, which interact with receptors expressed on the targeted cells. Targeting ligands which have been successfully utilized thus far include antibodies, peptides, aptamers, and carbohydrates (glycans).[22−26] The latter has come to the forefront of the scientific community in the past number of years with the discovery that glycans regulate numerous biological processes such as cell communication and selective binding of other biological species, among others, which makes glycochemistry an attractive tool in the design of materials for selective targeting.[27−29] In particular, complex (surface) glycoproteins are involved in biological binding events, and this has inspired research into the development of simplistic synthetic glycoprotein mimics.[30−37] Of particular attraction are glycopolypeptides derived from the polymerization of amino acid N-carboxyanhydrides (NCA) due to their ready availability and structural similarity to natural proteins.[38−48] The successful formulation of these glycopolypeptides into bioactive nanomaterials has been demonstrated albeit mostly by self-assembly.[49−51]

In this work we devise a novel one-step strategy to prepare glycosylated fluorescent polystyrene nanoparticles in a miniemulsion using glycosylated polypeptide−PS conjugates as macromolecular surfactants. Its attractiveness lies in the fact that the glycans play a large part in stabilizing the polymer latex while at the same time are presented at the final nanoparticle surface available for selective binding (Figure 1). The obtained
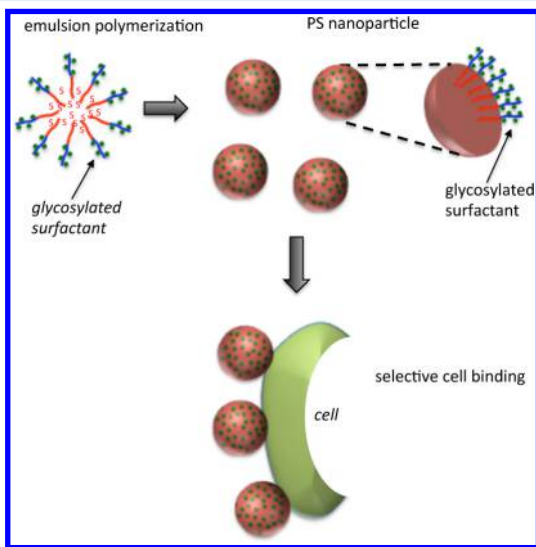

Figure 1. Schematic route for the synthesis of glycosylated poly(styrene) nanoparticles with selective binding properties.

PS NPs have a glycosylated periphery, which provides molecular recognition capabilities demonstrated by the specific binding to lectin and Chinese hamster ovary (CHO) cells.

■ EXPERIMENTAL SECTION

Materials. All chemicals were purchased from Sigma-Aldrich and used as received unless otherwise noted. γ-Benzyl-L-glutamate and ε-benzyloxycarbonyl-L-lysine were supplied by Bachem. Anhydrous dimethylformamide (DMF), chloroform, ethyl acetate, and methanol

were used directly from the bottle under an inert and dry atmosphere. γ-Benzyl-L-glutamate (BLG) and ε-benzyloxycarbonyl-L-lysine (ZLL) NCA were synthesized following a literature procedure.[52] Butyl phthalimidomethyl trithiocarbonate (RAFT CTA 1) and the PS homopolymer (PS TTC) were synthesized according to a literature procedure by Moad.[53]

Polystyrene−Trithiocarbonate (PS-TTC) Cleavage Using Bu₃SnH. PS−TTC (1) (2.5 g, 0.46 mmol) was dissolved in THF (15 mL) and added to a 50 mL round-bottomed flask equipped with a magnetic stirring bar. The mixture was degassed with nitrogen for 30 min before the addition of Bu₃SnH (1.03 mL, 3.8 mmol) and AIBN (0.19 g, 1.2 mmol). The reaction was left to stir for 3 h at 60 °C. The solution was purified by precipitation into a 400 mL 80/20 mixture of methanol/*n*-heptane under vigorous stirring. This was repeated and washed twice with the same mixture to remove any excess Bu₃SnH. The product was identified via ¹H NMR spectroscopy (CDCl₃). Isolated yield: 2.1 g.

Phthalimide Deprotection to Produce PS-NH₂ (2). Phthalimide end-functional polymer (1.7 g, 0.31 mmol) was dissolved in 10 mL of DMF and added to a 50 mL Schlenk tube equipped with a magnetic stirring bar. The reaction mixture was placed in a preheated oil bath of 70 °C and hydrazine monohydrate (0.28 mL, 20 mol equiv of hydrazine) added. The reaction mixture was stirred for 3 h. The solution was purified by precipitation into 300 mL of methanol and subsequently washed twice with methanol. The product was dried under high vacuum at 40 °C and isolated as a white powder. The product was identified by ¹H NMR spectroscopy (CDCl₃) (see Figure S1). M_w: 4800 g/mol, $Đ$ = 1.05, d*n*/d*c* = 0.159 mL/g. Isolated yield: 1.5 g.

General Procedure for the Synthesis of Hybrid Block Copolymers via NCA ROP. Chain extension of the PS-NH₂ macroinitiator was done according to a method described in previous work.[54] PS₄₅-*b*-PBLG₆₆: M_w: 18 200 g/mol, $Đ$ = 1.06, d*n*/d*c* = 0.192 mL/g (¹H NMR spectrum Figure S3, SEC Figure 2). PS₄₅-*b*-PZLL₇₃: M_w: 22 300 g/mol, $Đ$ = 1.07, d*n*/d*c* = 0.129 mL/g (¹H NMR spectrum Figure S3, SEC Figure S2).
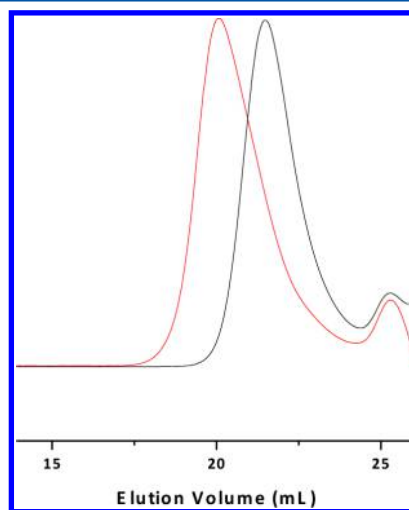

Figure 2. SEC traces of PS-NH₂ (**2**, black) and PS₄₅-*b*-PZLL₇₃ (**4**, red).

Polypeptide Deprotection. A general procedure was used for the deprotection of both the PBLG and PZLL pendant groups: PS₄₅-*b*-PBLG₆₆ (1.35 g, 7.4 × 10⁻⁵ mmol) was dissolved in trifluoroacetic acid (12 mL) and a minimal amount of THF to improve solubility. A solution of HBr (33 wt % in acetic acid) (3 mL, 15 mmol, 3-fold excess with respect to γ-benzyl-L-glutamate repeat units) was added slowly to the reaction at 0 °C. After 4 h, the solution was added to 200 mL of diethyl ether, and the precipitate was washed several times with diethyl ether. The subsequent product was redissolved in a 0.5 M NaOH solution (aqua) to obtain the polymer in the sodium salt form. The

sodium salt polymer was dialyzed against double deionized (DDI) water using Spectra/Por dialysis membranes (MWCO, 3.5 kDa) for 72 h at room temperature. The product was lyophilized and isolated as a white powder. Yield: 0.80 g, 6.1×10^{-5} mmol, 82% yield.

Glycosylation. *PS_{45}-b-($PLGA_{31}$-r-$GA_{35})_{66}$ (5).* Glycosylation of the carboxylic acid moieties was achieved according to a modified literature procedure.[43] PS_{45}-*b*-$PLGA_{66}$ (0.75 g, 5.7×10^{-5} mol) and galactosamine hydrochloride (0.43 g, 2.0 mmol, 33 equiv with respect to repeating units) were dissolved in deionized water (12 mL) and stirred for 15 min. 4-(4,6-Dimethoxy-1,3,5-triazin-2-yl)-4-methylmorpholinium chloride (DMT-MM) (0.55 g, 2.0 mmol, 1 equiv to galactosamine HCl) was dissolved in 5 mL of deionized water and added to the reaction mixture. After stirring for 24 h at room temperature the reaction mixture was dialyzed against DDI water using Spectra/Por dialysis membranes (MWCO, 3.5 kDa) for 72 h at room temperature. The polymer was subsequently lyophilized and isolated as a white powder. ^{1}H NMR spectrum: see Figure 3. Isolated yield: 1.1 g.
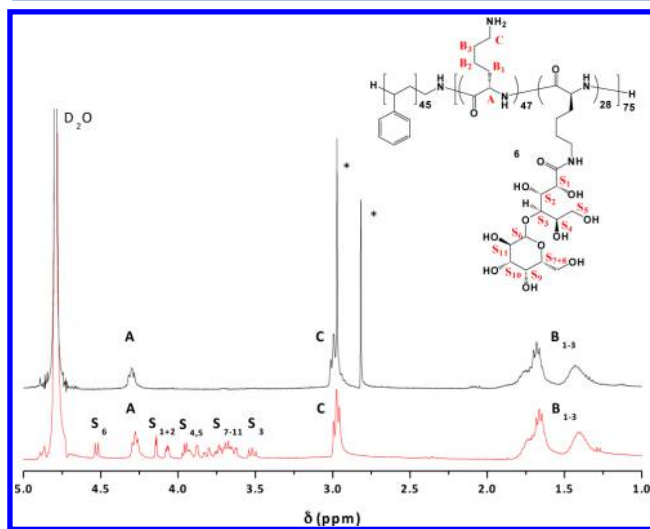

Figure 3. ^{1}H NMR spectra (in D_2O) of PS_{45}-*b*-PLL_{75} (top) and PS_{45}-*b*-(PLL_{46}-*r*-LA_{28}) (**6**) (bottom).

PS_{45}-b-(PLL_{47}-r-$LA_{28})_{75}$ (6). A general procedure for 1-ethyl-3-[3-(dimethylamino)propyl]carbodiimide hydrochloride (EDC)/*N*-hydroxysuccinimide (NHS) coupling was employed to attach lactobionic acid to the lysine residues of the amphiphile. Lactobionic acid (0.64 g, 1.8 mmol, 25 equiv with respect to repeat units), EDC (0.45 g, 2.3 mmol, 1.3 equiv), and NHS (0.43 g, 3.7 mmol, 2 equiv) were dissolved in 2 mL of 10 mM MES buffer (pH 4.7) and stirred for 20 min, and then PS_{45}-*b*-PLL_{73} (1 g, 7.2×10^{-5} mol in 8 mL of DDI water) added. The reaction mixture was stirred overnight. The resulting product was purified via dialysis against DDI water using Spectra/Por dialysis membranes (MWCO, 3.5 kDa) for 72 h at room temperature. The product was subsequently lyophilized and isolated as a white powder. ^{1}H NMR spectroscopy: see Figure S5. Isolated yield: 1.4 g.

Preparation of Polystyrene Nanoparticles via Emulsion Polymerization. Batch emulsion polymerizations of styrene were all carried in a three-neck reactor equipped with a reflux condenser, nitrogen inlet, and mechanical stirrer. A typical reaction proceeded as follows: PS_{45}-*b*-($PLGA_{31}$-*r*-GA_{35}) (0.25 g) was added to the reactor under an inert atmosphere and dissolved in 34 mL of distilled water under stirring at 70 °C. 4 mL of a sodium carbonate buffer solution (80 mg) was deoxygenated and injected into the reactor. The styrene monomer (4.80 g) was deoxygenated separately for 20 min by bubbling nitrogen through it and injected into the reactor. A deoxygenated initiator solution (50 mg of potassium persulfate in 2 mL of water) was injected to start the polymerization. The nitrogen flow was maintained throughout the reaction. Samples were withdrawn at regular times to determine the conversion. A small amount of

hydroquinone was added to these aliquots to quench the radical polymerization where the monomer conversion was then determined via gravimetry.

Nile Red Encapsulated NPs. Nile Red (NR) was encapsulated in the polystyrene nanoparticles by dissolving NR (0.1 wt % with regard to monomer) in the styrene monomer and subsequently forming the particles via an emulsion polymerization (as previously described).

PS_{45}-b-(PLL_{45}-r-LA_{26}-r-$FITC_2$). Fluorescein isothiocyanate (FITC) was attached to the lysine residues at 1.5 mol equiv per chain. FITC was dissolved in DMSO and added to PS_{45}-*b*-(PLL_{47}-*r*-$LA_{28})_{75}$ solubilized in PBS, pH 7.2. The resulting polymer was purified via dialysis against DDI water using Spectra/Por dialysis membranes (MWCO, 3.5 kDa) for 72 h and isolated as an orange powder.

Lectin Binding. The selective lectin−carbohydrate binding between the galactose moieties and RCA_{120} was done on a qualitative basis. After particle synthesis, the polystyrene latex was diluted with PBS buffer (pH 7.2), and a solution of the RCA_{120} lectin (1 mg/mL) was added until the system collapsed. The reversibility of the system was indicated via the addition of dissolved lactobionic acid in PBS buffer.

Cell Binding. Chinese hamster ovary (CHO) cells were seeded at 2×10^5 in 2 mL media on a 35 mm glass bottom culture dish for 24 h at 37 °C at 5% CO_2. The media were removed, and cells were washed with PBS (supplemented with 1.1 mM $MgCl_2$ and 0.9 mM $CaCl_2$). The particles were added to the cells in Phenol Red-free media (1:4 dilution) and were incubated for 2 h at 37 °C at 5% CO_2 in the dark. Cells were washed with 1 mM lactobionic acid in PBS for 15 min at 37 °C to assess displacement of any bound particles.

Methods. Nuclear magnetic resonance (NMR) spectra were recorded on a Bruker Avance 400 (400 MHz) in DMSO-d_6 and $CDCl_3$ as solvents. All chemical shifts are reported in parts per million (ppm) with tetramethylsilane (TMS) as an internal reference. Size exclusion chromatography (SEC) was performed on an Agilent 1200 system in conjunction with two PSS GRAM analytical (8×300 and 8×100, 10 μm) columns, a Wyatt Dawn Heleos 8 multiangle light scattering (MALS) detector, and a Wyatt Optilab rEX differential refractive index (DRI) detector with a 658 nm light source. The eluent was DMF containing 0.1 M LiBr at a flow rate of 1 mL/min. The column temperature was set to 40 °C with the MALS detector at 35 °C and the DRI detector at 40 °C. Molar masses and dispersities were calculated from the MALS signal by the Astra software (Wyatt) using the refractive index increment (dn/dc) as determined experimentally. The specific refractive index increments for the copolymers were calculated relative to the ratio of the homopolymer. The dn/dc values used for PS, PZLL, and PBLG were 0.159, 0.120, and 0.118 mL/g, respectively. All samples for SEC analysis were filtered through a 0.45 mm PTFE filter (13 mm, PP housing, Whatman) prior to injection. Dynamic light scattering (DLS) experiments were performed at 25 °C on a Malvern NanoZS (Malvern Instruments, Malvern UK) which uses a detection angle of 173° and a 3 mW He−Ne laser operating at a wavelength of 633 nm. The hydrodynamic diameter and polydispersity index (PDI) values were obtained using cumulated analysis. Field emission scanning electron microscopy (FESEM) images were obtained on a Hitachi S5500 SEM. Cells were imaged using a Zeiss LSM510 Meta confocal microscope using a 63× oil immersion objective lens and heated stage set to 37 °C. The particles were excited using 514 nm laser, and the emission collected using a long pass 560 nm filter set.

■ RESULTS AND DISCUSSION

Synthesis of Glycosylated Amphiphilic Block Copolymers. The synthesis of polypeptide−PS block copolymers was achieved following a strategy previously reported from our group by the macroinitiation of NCA ring-opening polymerization from amine-functional PS **2** obtained by reversible addition−fragmentation chain transfer (RAFT) polymerization (Scheme 1).[54] Briefly, a phthalimide protected amine is incorporated in a trithiocarbonate RAFT chain transfer agent

Scheme 1. Synthesis of Glycosylated Block Copolymers[a]
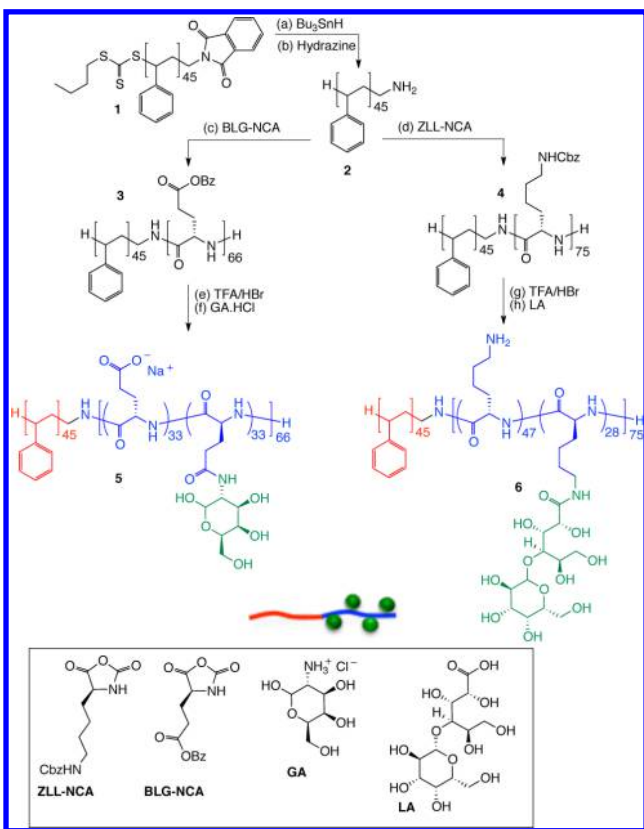
[a]Reagents and conditions: (a) Bu₃SnH (8 equiv), AIBN (3 equiv) THF, 60 °C; (b) NH₂NH₂ (20 equiv), DMF, 70 °C; (c) BLG-NCA (70 $[M]_0/[MI]_0$), DMF, HV, 0 °C; (d) ZLL-NCA (70 $[M]_0/[MI]_0$), DMF, HV, 0 °C; (e) HBr (33 wt % in AcOH), TFA; 0.5 M NaOH(aq); (f) DMT-MM, DDI; (g) HBr (33 wt % in AcOH), TFA; (h) LA, EDC/NHS, pH 4.7, 10 mM MES buffer; DDI. MI = macroinitiator, HV = high vacuum, DDI = distilled deionized water.

(CTA, **1**) which allows for effective control over the polymerization of styrenics. Tributyltin hydride in the presence of AIBN was used successfully to quantitatively remove the trithiocarbonate group.[54−56] Quantitative deprotection of the phthalimide protecting group followed on treatment with excess hydrazine monohydrate (Scheme 1 and Figure S1) resulting in the PS-NH₂ macroinitiator **2** (4700 g/mol, Đ = 1.1).

The subsequent NCA polymerizations were run at 0 °C under high vacuum to combine high polymerization control with efficient removal of the reaction byproduct CO₂ to accelerate the polymerization rate.[57,58] The PS-NH₂ macroinitiator was chain extended with ε-benzyloxycarbonyl-L-lysine (ZLL) and γ-benzyl-L-glutamate (BLG) NCAs where chain lengths of 70 repeat units were targeted (Scheme 1). A shift in the elution time in size exclusion chromatography (SEC) upon macroinitiation confirms the formation of the block copolymer with no residual homopolymer present highlighting efficient initiation (Figure 2 and Figure S2). Both block copolymers were further characterized using ¹H NMR, where comparison of the polypeptide protecting group signals with that of the characteristic aromatic polystyrene signals allowed determining the respective degrees of polymerization as summarized in Table 1 (Figure S3). For both block copolymers there is a good agreement between the monomer to macroinitiator feed ratio

Table 1. Characteristics of Poly(styrene) Macroinitiator (MI) and Block Copolymers

polymer[a]	$[NCA]_0/[MI]_0$	M_w[b] (g/mol)	Đ
PS₄₅-NH₂ (MI) **2**		4800	1.1
PS₄₅-b-PZLL₇₅ **4**	70	22300	1.1
PS₄₅-b-PBLG₆₆ **3**	70	18200	1.1

[a]Degree of polymerization was determined via ¹H NMR spectroscopy by calculating the ratio of styrene to polypeptide repeat units using the methylene protons of the polypeptide protecting group (5.0 ppm) to that of the combined signals of the aromatic protons of styrene and the polypeptide protecting group (6.2−7.5 ppm) (Figure S3). [b]Values obtained from multiangle light scattering (MALS) detection.

(70) and the calculated degree of polymerization (75 and 66, respectively).

After quantitative deprotection of the polypeptide block, galactose was covalently attached to the amino acid units via two different strategies targeting 35% and 50% glycosolation (Scheme 1) depending on the size of the sugar. A procedure described by Menzel[43] was employed to attach D-galactosamine (GA) to the carboxylic acid moieties of the PS₄₅-b-PLGA₆₆ to prepare PS₄₅-b-(PLGA₃₁-r-GA₃₅)₆₆ (**5**) (Figure S4). 4-(4,6-Dimethoxy-1,3,5-triazin-2-yl)-4-methylmorpholinium chloride (DMT-MM) is a mild and efficient amide-coupling agent, which was used to facilitate the reaction. DMT-MM allows for a high degree of substitution while it has been shown to be a very versatile component in preparing poly(glutamic acid) derivatives with orthogonal reactive sites.[59] For PS₄₅-b-PLL₇₅, EDC/NHS coupling chemistry was used to attach lactobionic acid (LA, 4-O-β-galactopyranosyl-D-gluconic acid, **7**) to the lysine residues typically targeting 35% glycosylation of the PLL block. LA is a readily available disaccharide with a galactose moiety and a cost-effective alternative to the functional sugars typically incorporated in other glycosylation strategies.

Emulsion Polymerization. Glycosylation of the polypeptide block permitted to impart certain traits necessary for the effective stabilization of the targeted polymer NPs. It was envisaged that by attaching highly water-soluble carbohydrate moieties the electrolytic nature of the polypeptide would decrease. At the same time, the effective range of macromolecular stabilization during the synthesis of the hydrophobic latex particles was expected to increase. To the best of our knowledge, glycosylated polypeptide hybrid block copolymers have not yet been investigated in emulsion polymerization.

The emulsion polymerization of styrene stabilized by either PS₄₅-b-(PLGA₃₁-r-GA₃₅)₆₆ **5** or PS₄₅-b-(PLL₄₇-r-LA₂₈)₇₅ **6** was carried out in order to evaluate the ability of the hybrid conjugates to form stable polystyrene nanoparticles with a brushlike periphery. All reactions were performed using potassium persulfate as a water-soluble initiator at 70 °C and a concentration of 1 wt % with respect to monomer (1 pphm). Monomer contents of 12 and 15 wt %, and block copolymer contents of 2 and 5 pphm were used for both block copolymers. In all but one experiment high styrene conversion and stable particle dispersion were obtained. Only in the case of using a low concentration of PS₄₅-b-(PLL₄₇-r-LA₂₈)₇₅ (i.e., 2 pphm) a stable latex could not obtain, which implies that PS₄₅-b-(PLGA₃₁-r-GA₃₅)₆₆ has better stabilizing properties than PS₄₅-b-(PLL₄₇-r-LA₂₈)₇₅. Conversion−time curves for the PS₄₅-b-(PLGA₃₁-r-GA₃₅)₆₆-stabilized emulsion polymerizations are shown in Figure 4.
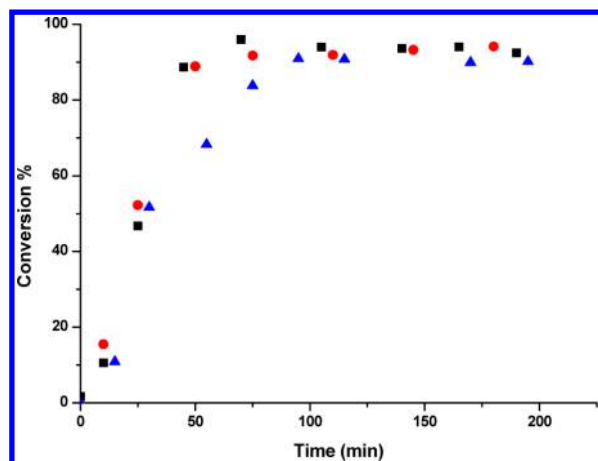
Figure 4. Evolution of monomer conversion with time for the emulsion polymerization of styrene using KPS as initiator (1 wt %), a monomer content of 12 wt % and surfactant content of 5 wt % (■), a monomer content of 15 wt % and surfactant content of 5 wt % (●), and a monomer content of 15 wt % and surfactant content of 2 wt % (▲) with PS_{45}-b-$(PLGA_{31}$-r-$GA_{35})$ as stabilizer.

All three curves show the absence of a nucleation period typical for a conventional *ab initio* emulsion polymerization. This behavior, which we observed before, suggests that the block copolymer micelles present at the start of the reaction act as a seed and are converted into particles.[60−63] Furthermore, it is clear from this figure that higher block copolymer concentrations lead to faster rates. This observation is consistent with the smaller particle diameters as determined using dynamic light scattering (Table 2) (Figure S5) for the

Table 2. Results from the Emulsion Polymerization of Styrene Using Glycosylated Block Copolymers as Surfactants

polymer	solid content[a] (wt %)	[polymer][b] (pphm)	$D_z{}^c$ (nm)	PDI[d]
PS_{45}-b-$(PLGA_{31}$-r-$GA_{35})_{66}$ **5**	12	5	114	0.02
PS_{45}-b-$(PLGA_{31}$-r-$GA_{35})_{66}$ **5**	15	5	120	0.02
PS_{45}-b-$(PLGA_{31}$-r-$GA_{35})_{66}$ **5**	15	2	147	0.02
PS_{45}-b-$(PLL_{47}$-r-$LA_{28})_{75}$ **6**	12	5	111	0.06
PS_{45}-b-$(PLL_{47}$-r-$LA_{28})_{75}$ **6**	15	5	119	0.04
PS_{45}-b-$(PLL_{47}$-r-$LA_{28})_{75}$ **6**	15	2	n/a	n/a

[a]Solid content = mass polymer/mass dispersion. [b]1 pphm = 1 g block copolymer/100 g monomer. [c]Z-average particle diameter from dynamic light scatering (DLS). [d]Polydispersity Index of particle size distribution from cumulative DLS analysis.

higher block copolymer concentrations; smaller diameters imply larger particle numbers, which in turn lead to higher polymerization rates. The increase in monomer content while maintaining a constant surfactant/monomer ratio does not significantly affect either particle size (Table 2) or the polymerization rate (Figure 4), implying that in both cases very similar particles are produced, i.e., particles of the same size and same glycopolymer periphery. These results, in combination with the narrow particle size distributions (PDI < 0.02, Table 2), clearly demonstrate the high amount of control over particle synthesis with these block copolymer surfactants.

In the case of PS_{45}-b-$(PLL_{47}$-r-$LA_{28})_{75}$ **6** as the macromolecular surfactant, it was found that the stabilization was not

as effective as for PS_{45}-b-$(PLGA_{31}$-r-$GA_{35})_{66}$ **5**; only at block copolymer contents of 5 pphm stable dispersions were obtained. Interestingly, at block copolymer contents of 5 pphm both block copolymers seem to be able to stabilize very similar particle surface areas as can be concluded from the similar particle diameters listed in Table 2 (also see Figures S6 and S7). All particles were further investigated with FE-SEM highlighting the uniformity of the particles, all ranging between 80 and 90 nm in diameter (Figure 5).
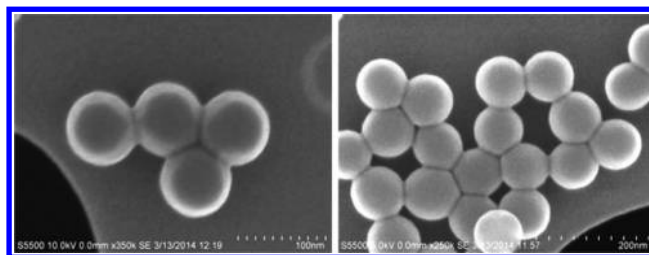

Figure 5. FE-SEM images of polystyrene latex stabilized by PS_{45}-b-$(PLGA_{31}$-r-$GA_{35})_{66}$ (**5**) with a monomer content of 12 wt % and surfactant content of 5 wt % (Table 2).

Selective Binding of Fluorescent NPs. Various methods are available to prepare functional polystyrene microspheres, where the most common method would arguably be to engineer functional layers on existing microspheres by postmodification.[64,65] Divinylbenzene (DVB) and ethylene glycol dimethacrylate (EGDMA) are typically incorporated to cross-link the PS particle, resulting in free vinyl groups at the surface. Surface modification using thiol−ene chemistry can then be utilized to introduce glyco-functionalities as was demonstrated on microspheres by Alvarez-Paino.[66]

The use of functional macromolecular surfactants during an emulsion polymerization of hydrophobic monomer allows for a straightforward strategy to functional polymer NPs. Furthermore, the introduction of fluorescent tags to track the polystyrene particles as they target specific biological entities can readily be achieved. This is demonstrated using two different strategies. In the first instance a highly hydrophobic dye, Nile Red, was incorporated during the emulsion polymerization of styrene at 0.1 wt % with regards to the monomer. Figure 6A depicts the PS particles stabilized by PS_{45}-b-$(PLGA_{31}$-r-$GA_{35})_{66}$ in water under UV light. Here the incorporation of NR is evident as well as the effective stabilization due to the glycosylated hydrophilic shell. After the addition of a galactose binding lectin, RCA_{120}, multivalent binding between the lectin and the galactose functional NPs results in the precipitation of the whole system (Figure 6B).
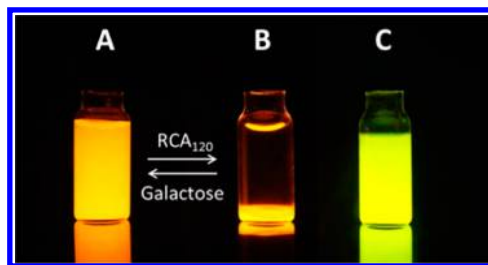

Figure 6. Image of Nile Red encapsulated PS_{45}-b-$(PLGA_{31}$-r-$GA_{35})$ stabilized PS NPs in water before (A) and after (B) the addition of the lectin RCA_{120}. PS_{45}-b-$(PLL_{45}$-r-LA_{26}-r-$FITC_2)$ is represented by (C).
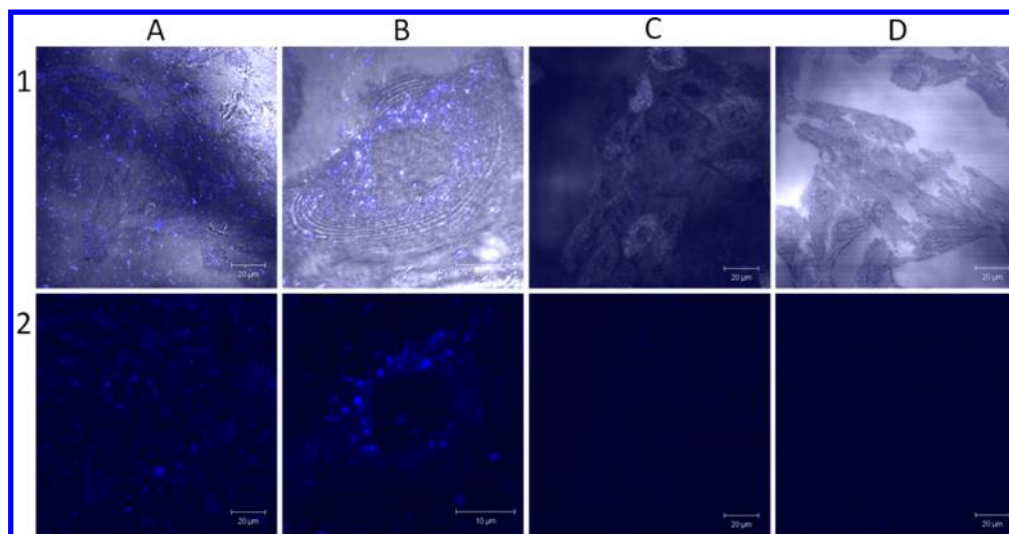
Figure 7. Confocal fluorescence imaging showing binding of PS_{45}-b-$(PLGA_{31}$-r-$GA_{35})$ nanoparticles (1:4 dilution) to live CHO cells following a 2 h incubation at 37 °C (2A) where (2B) expands a single cell image to show the distribution of particles at the cell surface ($z = 3.5$). (1A) and (1B) show the reflectance images of the cells superimposed on the fluorescence images. (2C) shows the fluorescence images of the CHO cells treated with the nanoparticles; after they had been washed with 1 mM lactobionic acid in PBS for 15 min at 37 °C, the absence of fluorescence confirmed binding was reversed. (2D) shows that following incubation with 300 μM lactobionic acid for 1 h, prior to the addition of nanoparticles (1:4 dilution) for 2 h, no particle binding occurred. (1C) and (1D) show the reflectance images for these studies superimposed on the fluorescence images to confirm that the cells were present but unmodified by the particles.

The effects are however reversible as the addition of excess lactobionic acid and thus competing galactose moieties allow the system to revert to the original stabilized state. The same was observed for the system incorporating PS_{45}-b-$(PLL_{47}$-r-$LA_{28})_{75}$ (Figure S8).

In a second system, the excess lysine residues of PS_{45}-b-$(PLL_{47}$-r-$LA_{28})_{75}$ was utilized to prepare fluorescein-labeled PS particles. The reactivity of fluorescein isothiocyanate (FITC) toward primary amines is well-known, and thus the synthesis of PS_{45}-b-$(PLL_{45}$-r-LA_{28}-r-$FITC_2)_{75}$ is a facile approach to fluorescent PS particles. Subsequently, PS_{45}-b-$(PLL_{45}$-r-LA_{28}-r-$FITC_2)_{75}$ was used to stabilize the emulsion polymerization of styrene to produce fluorescent glycosylated PS particles (Figure 6C).

These results demonstrate the feasibility of the proposed approach allowing two methods of labeling, i.e., in the NP core and the periphery by simple chemistry. While this was not further pursuit here, this would allow the introduction of two different labels for imaging. Such an approach is potentially of significant value in fluorescence sensing applications where two probes are used to permit referencing of the transduction signal by an analytically inert probe. Such an approach has been described for dye encapsulation, for example in silicate or polystyrene spheres but the advantage of this approach is that the probes are physically separated between core and shell of the nanoparticle, which can reduce potential probe cross-talk.[67]

While lectine binding experiments provide a conceptional proof for selective binding, *in vitro* cellular binding of the nanoparticles was investigated in CHO cells. Carbohydrate receptors such as lectins are prevalent on cell surfaces, and CHO-K1 was used in the present study because this cell line has been demonstrated previously to express relatively large amounts of Galectin 1, which resides at the plasma membrane and can bind to extracellular glycoconjugate ligands.[68,69] Figure 7 shows confocal images of live CHO cells following 2 h incubation with 1:4 PS_{45}-b-$(PLGA_{31}$-r-$GA_{35})_{66}$ **5** nanoparticles in cell media (A and B). It was found that the particles bound

strongly to the cell surface and remained bound after washing several times with PBS (supplemented with 0.9 mM $CaCl_2$ and 1.1 mM $MgCl_2$). Using confocal imaging, scanning in the Z-direction, it was confirmed that the particles did not permeate the cells.

To confirm surface binding was specific, lactobionic acid containing a galactose moiety was used in order to remove any specifically bound particles on the cell surface. This was achieved by incubating CHO cells with 1 mM lactobionic acid in PBS for 15 min at 37 °C. The media were removed from the cells, and they were washed with PBS buffer (supplemented with 0.9 mM $CaCl_2$ and 1.1 mM $MgCl_2$). Figure 7C shows that particles were displaced by the wash step with lactobionic acid.

To assess if the binding process to the cell surface could be blocked, CHO cells were incubated with 300 μM lactobionic acid in cell media for 1 h at 37 °C, and particles were added to give final concentration of a 1 in 4 dilution, for a further 2 h. Figure 7D confirmed that the particles could not bind to the cell surface in the presence of lactobionic acid. It is important to note that in the control described above where the cells were washed extensively with PBS buffer in the absence of lactobionic acid, the particles remained bound to the cell surface; i.e., they were not removed by washing. These results indicate that the galactose modified particles bound in a receptor specific way to the cell surface.

■ CONCLUSIONS

Hybrid block copolymers consisting of poly(styrene) and a poly(amino acid) segments were synthesized via combination of RAFT and NCA polymerization. The polypeptide segments were glycosolated with galactose moieties using traditional coupling chemistry. The resulting amphiphilic block copolymers were found to be efficient stabilizers in the emulsion polymerization of styrene, offering a facile method for the synthesis of fluorescent glycosylated polystyrene nanoparticles. The availability of the galactose units introduced through the glycopolymer surfactant at the nanoparticles surface for

selective binding was successfully demonstrated by lectin binding experiments and binding to Chinese hamster ovary (CHO) cells. This approach provides a straightforward route to highly fluorescent nanoparticles with selective binding properties with potential for bioimaging applications.

■ ASSOCIATED CONTENT

S **Supporting Information**

Experimental procedures; ^{1}H NMR spectra; SEC traces; DLS of nanoparticles. This material is available free of charge via the Internet at http://pubs.acs.org.

■ AUTHOR INFORMATION

Corresponding Author

*E-mail andreas.heise@dcu.ie (A.H.).

Notes

The authors declare no competing financial interest.

■ ACKNOWLEDGMENTS

■ REFERENCES

(1) Elsabahy, M.; Wooley, K. L. *Chem. Soc. Rev.* **2012**, *41*, 2545.

(2) Parveen, S.; Misra, R.; Sahoo, S. K. *J. Nanomed. Nanotechnol.* **2012**, *8*, 147.

(3) Ryu, J. H.; Koo, H.; Sun, I.-C.; Yuk, S. H.; Choi, K.; Kim, K.; Kwon, I. C. *Adv. Drug Delivery Rev.* **2012**, *64*, 1447.

(4) Vollrath, A.; Schubert, S.; Schubert, U. S. *J. Mater. Chem. B* **2013**, *1*, 1994.

(5) Gupta, A. K.; Gupta, M. *Biomaterials* **2005**, *26*, 3995.

(6) Maeng, J. H.; Lee, D.-H.; Jung, K. H.; Bae, Y.-H.; Park, I.-S.; Jeong, S.; Jeon, Y.-S.; Shim, C.-K.; Kim, W.; Kim, J.; Lee, J.; Lee, Y.-M.; Kim, J.-H.; Kim, W.-H.; Hong, S.-S. *Biomaterials* **2010**, *31*, 4995.

(7) Borase, T.; Ninjbadgar, T.; Kapetanakis, A.; Roche, S.; O'Connor, R.; Kerskens, C.; Heise, A.; Brougham, D. F. *Angew. Chem., Int. Ed.* **2013**, *52*, 3164.

(8) Santra, S.; Dutta, D.; Walter, G. A.; Moudgil, B. M. *Technol. Cancer Res. Treat.* **2005**, *4*, 593.

(9) Santra, S.; Malhotra, A. *WIRES Nanomed. Nanobi.* **2011**, *3*, 501.

(10) Ow, H.; Larson, D. R.; Srivastava, M.; Baird, B. A.; Webb, W. W.; Wiesner, U. *Nano Lett.* **2004**, *5*, 113.

(11) Kamaly, N.; Xiao, Z.; Valencia, P. M.; Radovic-Moreno, A. F.; Farokhzad, O. C. *Chem. Soc. Rev.* **2012**, *41*, 2971.

(12) Mai, Y.; Eisenberg, A. *Chem. Soc. Rev.* **2012**, *41*, 5969.

(13) Friedrich, H.; McKenzie, B.; Bomans, P. H. H.; Deng, Z.; Nudelman, F.; Holder, S. J.; de With, G.; Somerdijk, N. *Microsc. Microanal.* **2010**, *16*, 832.

(14) Rösler, A.; Vandermeulen, G. W. M.; Klok, H.-A. *Adv. Drug Delivery Rev.* **2012**, *64*, 270.

(15) Danhier, F.; Ansorena, E.; Silva, J. M.; Coco, R.; Le Breton, A.; Preat, V. *J. Controlled Release* **2012**, *161*, 505.

(16) Owens, D. E., III; Peppas, N. A. *Int. J. Pharm.* **2006**, *307*, 93.

(17) Ma, Y.; Sadoqi, M.; Shao, J. *Int. J. Pharm.* **2012**, *436*, 25.

(18) Sakuma, S.; Kataoka, M.; Higashino, H.; Yano, T.; Masaoka, Y.; Yamashita, S.; Hiwatari, K.-I.; Tachikawa, H.; Kimura, R.; Nakamura, K.; Kumagai, H.; Gore, J. C.; Pham, W. *Eur. J. Pharm. Sci.* **2011**, *42*, 340.

(19) Holzapfel, V.; Musyanovych, A.; Landfester, K.; Lorenz, M. R.; Mailänder, V. *Macromol. Chem. Phys.* **2005**, *206*, 2440.

(20) Albanese, A.; Tang, P. S.; Chan, W. C. W. *Annu. Rev. Biomed. Eng.* **2012**, *14*, 1.

(21) Caruso, F.; Stayton, P.; Ward, M. D. *Chem. Mater.* **2012**, *24*, 727.

(22) Dhar, S.; Gu, F. X.; Langer, R.; Farokhzad, O. C.; Lippard, S. J. *Proc. Natl. Acad. Sci. U. S. A.* **2008**, *105*, 17356.

(23) Singh, K.; Choudhary, M.; Chianella I.; Singh, P. *Adv. Nanopart.* **2013**, *182*.

(24) Ruoslahti, E. *Adv. Mater.* **2012**, *24*, 3747.

(25) Medley, C. D.; Bamrungsap, S.; Tan, W.; Smith, J. E. *Anal. Chem.* **2011**, *83*, 727.

(26) Yu, B.; Tai, H. C.; Xue, W.; Lee, L. J.; Lee, R. J. *Mol. Membr. Biol.* **2010**, *27*, 286.

(27) Cummings, R. D.; Pierce, J. M. *Chem. Biol.* **2014**, *21*, 1.

(28) Hudak, J. E.; Bertozzi, C. R. *Chem. Biol.* **2014**, *21*, 16.

(29) Lowary, T. L. *Curr. Opin. Chem. Biol.* **2013**, *17*, 990.

(30) Gamblin, D. P.; Scanlan, E. M.; Davis, B. G. *Chem. Rev.* **2008**, *109*, 131.

(31) Ting, S. R. S.; Chen, G.; Stenzel, M. H. *Polym. Chem.* **2010**, *1*, 1392.

(32) Spain, S. G.; Cameron, N. R. *Polym. Chem.* **2011**, *2*, 60.

(33) Spain, S. G.; Gibson, M. I.; Cameron, N. R. *J. Polym. Sci., Part A: Polym. Chem.* **2007**, *45*, 2059.

(34) Kiessling, L. L.; Gestwicki, J. E.; Strong, L. E. *Angew. Chem., Int. Ed.* **2006**, *45*, 2348.

(35) Huang, J.; Zhang, Q.; Li, G.-Z.; Haddleton, D. M.; Wallis, R.; Mitchell, D.; Heise, A.; Becer, C. R. *Macromol. Rapid Commun.* **2013**, *34*, 1542.

(36) Zhang, Q.; Collins, J.; Anastasaki, A.; Wallis, R.; Mitchell, D. A.; Becer, C. R.; Haddleton, D. M. *Angew. Chem., Int. Ed.* **2013**, *52*, 4435.

(37) Becer, C. R. *Macromol. Rapid Commun.* **2012**, *33*, 742.

(38) Kramer, J. R.; Deming, T. J. *J. Am. Chem. Soc.* **2010**, *132*, 15068.

(39) Huang, J.; Heise, A. *Chem. Soc. Rev.* **2013**, *42*, 7373.

(40) Krannig, K.-S.; Schlaad, H. *J. Am. Chem. Soc.* **2012**, *134*, 18542.

(41) Krannig, K.-S.; Huang, J.; Heise, A.; Schlaad, H. *Polym. Chem.* **2013**, *4*, 3981.

(42) Tang, H.; Zhang, D. *Biomacromolecules* **2010**, *11*, 1585.

(43) Mildner, R.; Menzel, H. *J. Polym. Sci., Part A: Polym. Chem.* **2013**, *51*, 3925.

(44) Huang, J.; Habraken, G.; Audouin, F.; Heise, A. *Macromolecules* **2010**, *43*, 6050.

(45) Xiao, C.; Zhao, C.; He, P.; Tang, Z.; Chen, X.; Jing, X. *Macromol. Rapid Commun.* **2010**, *31*, 991.

(46) Kramer, J. R.; Deming, T. J. *Polym. Chem.* **2014**, *5*, 671.

(47) Bonduelle, C.; Lecommandoux, S. *Biomacromolecules* **2013**, *14*, 2973.

(48) Krannig, K.-S.; Doriti, A.; Schlaad, H. *Macromolecules* **2014**, *47*, 2536.

(49) Huang, J.; Bonduelle, C.; Thevenot, J.; Lecommandoux, S.; Heise, A. *J. Am. Chem. Soc.* **2012**, *134*, 119.

(50) Bonduelle, C.; Mazzaferro, S.; Huang, J.; Lambert, O.; Heise, A.; Lecommandoux, S. *Faraday Discuss.* **2013**, *166*, 137.

(51) Bonduelle, C.; Huang, J.; Mena-Barragan, T.; Ortiz Mellet, C.; Decroocq, C.; Etame, E.; Heise, A.; Compain, P.; Lecommandoux, S. *Chem. Commun.* **2014**, *50*, 3350.

(52) Habraken, G. J. M.; Peeters, M.; Dietz, C. H. J. T.; Koning, C. E.; Heise, A. *Polym. Chem.* **2010**, *1*, 514.

(53) Postma, A.; Davis, T. P.; Evans, R. A.; Li, G.; Moad, G.; O'Shea, M. S. *Macromolecules* **2006**, *39*, 5293.

(54) Jacobs, J.; Gathergood, N.; Heise, A. *Macromol. Rapid Commun.* **2013**, *34*, 1325.

(55) Xu, J.; He, J.; Fan, D.; Wang, X.; Yang, Y. *Macromolecules* **2006**, *39*, 8616.

(56) Boyer, C.; Granville, A.; Davis, T. P.; Bulmus, V. *J. Polym. Sci., Part A: Polym. Chem.* **2009**, *47*, 3773.

(57) Vayaboury, W.; Giani, O.; Cottet, H.; Deratani, A.; Schué, F. *Macromol. Rapid Commun.* **2004**, *25*, 1221.

(58) Habraken, G. J. M.; Wilsens, K. H. R. M.; Koning, C. E.; Heise, A. *Polym. Chem.* **2011**, *2*, 1322.

(59) Barz, M.; Duro-Castano, A.; Vicent, M. J. *Polym. Chem.* **2013**, *4*, 2989.

(60) Munoz-Bonilla, A.; van Herk, A. M.; Heuts, J. P. A. *Macromolecules* **2010**, *43*, 2721.

(61) Munoz-Bonilla, A.; van Herk, A. M.; Heuts, J. P. A. *Polym. Chem.* **2010**, *1*, 624.

(62) Munoz-Bonilla, A.; Ali, S. I.; del Campo, A.; Fernandez-Garcia, M.; van Herk, A. M.; Heuts, J. P. A. *Macromolecules* **2011**, *44*, 4282.

(63) Rager, T.; Meyer, W. H.; Wegner, G.; Mathauer, K.; Mächtle, W.; Schrof, W.; Urban, D. *Macromol. Chem. Phys.* **1999**, *200*, 1681.

(64) Kawaguchi, H. *Prog. Polym. Sci.* **2000**, *25*, 1171.

(65) Goldmann, A. S.; Barner, L.; Kaupp, M.; Vogt, A. P.; Barner-Kowollik, C. *Prog. Polym. Sci.* **2012**, *37*, 975.

(66) Alvarez-Paino, M.; Munoz-Bonilla, A.; Marcelo, G.; Rodriguez-Hernandez, J.; Fernandez-Garcia, M. *Polym. Chem.* **2012**, *3*, 3282.

(67) Wang, X.-D.; Gorris, H. H.; Stolwijk, J. A.; Meier, R. J.; Groegel, D. B. M.; Wegener, J.; Wolfbeis, O. S. *Chem. Sci.* **2011**, *2*, 901.

(68) Cho, M.; Cummings, R. D. *J. Biol. Chem.* **1995**, *270*, 5198.

(69) Cho, M.; Cummings, R. D. *J. Biol. Chem.* **1995**, *270*, 5207.